PHYSICAL REVIEW E **66**, 040702(R) (2002)

Chaotic orientational behavior of a nematic liquid crystal subjected to a steady shear flow

Götz Rienäcker,[1] Martin Kröger,[1,2,3] and Siegfried Hess[1,2,*]
[1]*Institut für Theoretische Physik, Technische Universität Berlin, Fakultät II, Hardenbergstrasse 36, D-10623 Berlin, Germany*
[2]*Institute for Theoretical Physics, University of California Santa Barbara, California 93106-4030*
[3]*Polymer Physics, Material Sciences, ETH Zürich, CH-8092 Zürich, Switzerland*
(Received 12 April 2002; published 29 October 2002)

Based on a relaxation equation for the second rank alignment tensor characterizing the molecular orientation in liquid crystals, we report on a number of symmetry-breaking transient states and simple periodic and irregular, chaotic out-of-plane orbits under steady flow. Both an intermittency route and a period-doubling route to chaos are found for this five-dimensional dynamic system in a certain range of parameters (shear rate, tumbling parameter at isotropic-nematic coexistence, and reduced temperature). A link to the corresponding rheochaotic states, present in complex fluids, is made.

DOI: 10.1103/PhysRevE.66.040702 PACS number(s): 61.30.Gd, 61.30.Cz

A nematic liquid crystal (LC) subjected to a steady shear flow can either go to a stationary flow aligned state or respond with a time dependent molecular orientation depending on the magnitude of the tumbling parameter λ [1–3]. Both flow alignment and time dependent orientation, frequently referred to as ''tumbling'' behavior are observed in thermotropic, lyotropic, and polymeric LC's [4] In the tumbling regime, however, the dynamics are more complex than the Ericksen-Leslie director theory can describe. The second alignment tensor is needed to characterize the molecular orientation. Detailed theoretical studies [5], based on the solutions of a generalized Fokker-Planck equation [6,7], revealed that in addition to the tumbling motion, wagging and kayaking types of motions, as well as combinations thereof occur. Recently, also chaotic motions were inferred from a moment approximation to the Fokker-Planck equation leading to a 65-dimensional dynamical system [8] for uniaxial particles. While we consider uniaxial particles in this note, one may notice that for long triaxial ellipsoidal non-Brownian particles chaotic behavior had also been predicted in Ref. [9]. Here we report on our discovery [10] that a closed nonlinear relaxation equation for the alignment tensor, being equivalent to a five-dimensional dynamical system and strongly related to the full Fokker-Planck equation, leads to a chaotic behavior for particular values of the tumbling parameter and in certain ranges of the shear rate. Both the frequency doubling route, as in Ref. [8], and the intermittency route to chaos are found for the simpler system. Due to the coupling between the alignment and stress tensor (a relationship is given below), one may attempt to model the time dependent and also chaotic rheological behavior seen in the recent experiments on micellar materials [11], dense lamellar phases [12], and dense suspensions [13]—and discussed in more general theoretical considerations on rheochaos [14]—by variants of the dynamic system to be characterized in this paper. An illustrative example is given in Ref. [15], where equations similar to the one to be discussed below were used to describe the effect of (nonchaotic) shear thickening.

The molecular orientation is characterized by the second rank alignment tensor $\mathbf{a} \propto \langle \overline{\mathbf{uu}} \rangle$, where $\mathbf{u}$ is a unit vector parallel to the figure axis of an effectively uniaxial particle, or to a straight segment of a polymer chain or of a wormlike micelle. The symbol $\overline{\ldots}$ refers to the symmetric traceless part of a tensor and the brackets $\langle \cdots \rangle$ indicate an average to be evaluated with an orientational distribution function. Birefringence, i.e., the dielectric tensor is linked with $\mathbf{a}$, having symmetry properties of a quadrupole moment tensor. For a fluid subjected to a shear flow with the velocity gradient $\nabla \mathbf{v}$, where $\omega = (1/2)\nabla \times \mathbf{v}$ is the vorticity of the flow, the equation of change for the alignment tensor to be studied here is

$$\tau_a(\partial \mathbf{a}/\partial t - 2\overline{\omega \times \mathbf{a}}) + \mathbf{\Phi}(\mathbf{a}) = -\sqrt{2}\tau_{ap}\overline{\nabla \mathbf{v}}. \qquad (1)$$

The quantity $\mathbf{\Phi}$, specified below, is the derivative of a Landau-de Gennes free energy Φ with respect to the alignment tensor, it contains terms of first, second, and third order in $\mathbf{a}$. The equation stated here was first derived within the framework of irreversible thermodynamics [16], where the relaxation time coefficients $\tau_a > 0$ and τ_{ap} are considered as phenomenological parameters. It had been shown in Refs. [6,17] that τ_a and τ_{ap} are proportional to the Ericksen-Leslie viscosity coefficients γ_1 and γ_2, respectively. The basic equation used here can also be derived, within certain approximations, from a Fokker-Planck equation for the orientational distributions function that contains a torque associated with the molecular field proportional to $\mathbf{a}$ [6,7,18]. Then τ_a and the ratio $-\tau_{ap}/\tau_a$ can be related to the rotational diffusion coefficent and to a nonsphericity parameter associated with the shape of a particle. Equation (1) is applicable to both the isotropic and the nematic phases. Limiting cases that follow from this equation are the pretransitional behavior of the flow birefringence [19,20] in the isotropic phase [$\Phi(\mathbf{a})$ is approximated by its term linear in $\mathbf{a}$] and the Ericksen-Leslie theory in the uniaxial nematic phase. In the latter case, the Ericksen-Leslie viscosity coefficients γ_1 and γ_2 are proportional to τ_a and τ_{ap}, respectively, and $\lambda = -\gamma_2/\gamma_1$. Equation (1) has been applied to the study of the influence of a shear flow on the isotropic-nematic phase transition [19,20], and discussed intensively in recent, in particular, experimental works, see e.g., Refs. [3,4] and references cited therein.

*Corresponding author.

 ©2002 The American Physical Society

To proceed, we consider a plane Couette flow with the shear rate $\dot{\gamma}$, where velocity is in the x direction and gradient is in the y direction, i.e., $\overline{\nabla \mathbf{v}} = \dot{\gamma}\overline{\mathbf{e}^x\mathbf{e}^y}$ and $\omega = (-\dot{\gamma}/2)\mathbf{e}^z$. The alignment tensor $\mathbf{a}$ is expanded with respect to a complete set of five orthonormal basis tensors defined by $\mathsf{T}^0 = \sqrt{3/2}\overline{\mathbf{e}^z\mathbf{e}^z}$, $\mathsf{T}^1 = \sqrt{1/2}(\mathbf{e}^x\mathbf{e}^x - \mathbf{e}^y\mathbf{e}^y)$, $\mathsf{T}^2 = \sqrt{2}\overline{\mathbf{e}^x\mathbf{e}^y}$, $\mathsf{T}^3 = \sqrt{2}\overline{\mathbf{e}^x\mathbf{e}^z}$, $\mathsf{T}^4 = \sqrt{2}\overline{\mathbf{e}^y\mathbf{e}^z}$, i.e., $\mathsf{T}^i:\mathsf{T}^j = \delta^{ij}$, as $\mathbf{a} = \Sigma_i a_i \mathsf{T}^i$ with $a^2 \equiv \mathbf{a}:\mathbf{a} = \Sigma_i a_i^2$. In the following, the components a_i are expressed in units of the magnitude $\sqrt{5}S_K$ of the equilibrium alignment at the temperature T_K (or concentration c_K), where the nematic phase of a lyotropic LC coexists with its isotropic phase, S_K stands for the Maier-Saupe order parameter at coexistence. The pseudo-critical value where the term linear in $\mathbf{a}$, in the expression for $\mathbf{\Phi}$, vanishes is denoted by T^* (or c^*). One has $T^* < T_K$ (or $c^* > c_K$). The quantity $\delta_K = 1 - T^*/T_K$ (or $\delta_K = 1 - c_K/c^*$) is typically of the order of 1/10–1/100. It sets a reference scale for temperature (concentration) differences. A dimensionless relative temperature (concentration) variable is defined by $\vartheta = (1 - T^*/T)/\delta_K$ or $\vartheta = (1 - c/c^*)/\delta_K$. Then the Landau-de Gennes free energy assumes a simple form involving just the one model parameter ϑ, viz., $2\Phi = \vartheta a^2 - 2I^{(3)} + a^4$. Here $I^{(3)} = \sqrt{6}\ \mathrm{tr}(\mathbf{a}\cdot\mathbf{a}\cdot\mathbf{a})$ is the third-order scalar invariant. The scaled equilibrium alignment in the nematic phase, for $\vartheta < 1$, is $a_{eq} = a_{eq}(\vartheta) = [3 + (9 - 8\vartheta)^{1/2}]/4$. Clearly, $a_{eq} = 1$ at $\vartheta = 1$, corresponding to the equilibrium coexistence state point. The nematic and the isotropic phases are metastable in the intervals $1 < \vartheta < 9/8$ and $0 < \vartheta < 1$. Times are expressed in units of the relaxtion time $\tau_K = \tau_a/\delta_K$ of the alignment in the isotropic phase at the coexistence state or, equivalently, are related to the viscosity coefficient γ_1 of the nematic phase at coexistence by $\tau_K = \gamma_1/(15nk_BT_KS_K^2\delta_K)$, where n denotes number density. Shear rates are in units of τ_K^{-1}. Then Eq. (1) is equivalent to

$$\dot{a}_0 = -\Phi_0, \quad \dot{a}_1 = -\Phi_1 + \dot{\gamma}a_2, \quad \dot{a}_3 = -\Phi_3 + \tfrac{1}{2}\dot{\gamma}a_4, \quad (2)$$

$$\dot{a}_2 = -\Phi_2 - \dot{\gamma}a_1 - \frac{\dot{\gamma}\lambda_k\sqrt{3}}{2}, \quad \dot{a}_4 = -\Phi_4 - \tfrac{1}{2}\dot{\gamma}a_3. \quad (3)$$

The derivatives of the potential function with respect to the components of the alignment tensor are given by $\Phi_0 = \vartheta_0 a_0 + 3(a_1^2 + a_2^2) - (3/2)(a_3^2 + a_4^2)$, $\Phi_1 = \vartheta_1 a_1 - (3/2)\sqrt{3}(a_3^2 - a_4^2)$, $\Phi_2 = \vartheta_1 a_2 - 3\sqrt{3}a_3a_4$, $\Phi_3 = \vartheta_0 a_3 - 3\sqrt{3}(a_1a_3 + a_2a_4)$, and $\Phi_4 = \vartheta_0 a_4 - 3\sqrt{3}(a_2a_3 - a_1a_4)$, where the abbreviation $\vartheta_i \equiv \vartheta + (9i - 3)a_0 + 2a^2$ $(i = 0,1)$ is used. The dynamical system (2),(3) contains three control parameters two of which are determined by the state point and the material chosen, viz, ϑ and $\lambda_k = -2\sqrt{3}\tau_{ap}/(\sqrt{5}S_K\tau_a)$, which is the value of the tumbling parameter at phase coexistence. The actual tumbling parameter at a state point with $\vartheta < 1$ is $\lambda_{eq} = \lambda_k/a_{eq}$. The third control parameter is the shear rate $\dot{\gamma}$.

The components $a_{0,1,2}$ are linked with symmetry of the plane Couette flow. According to Eq. (3), $a_{3,4}$ remain zero when they are zero initially. It seemed sufficient [19–22] to study the smaller system (2) involving three components just as one deals with three components of shear stress tensor, viz., the shear stress and two normal stress differences. Equation (2) with $a_{3,4} = 0$ decribes correctly the flow aligned state as well as the tumbling and wagging behavior of the full system for certain ranges of control parameters. In this paper, we report on the symmetry-breaking solutions with $a_{3,4} \neq 0$, which exist in some specific ranges of the control parameters. These solutions are associated with kayaking types of motions, but also rather complex and chaotic orbits are found.

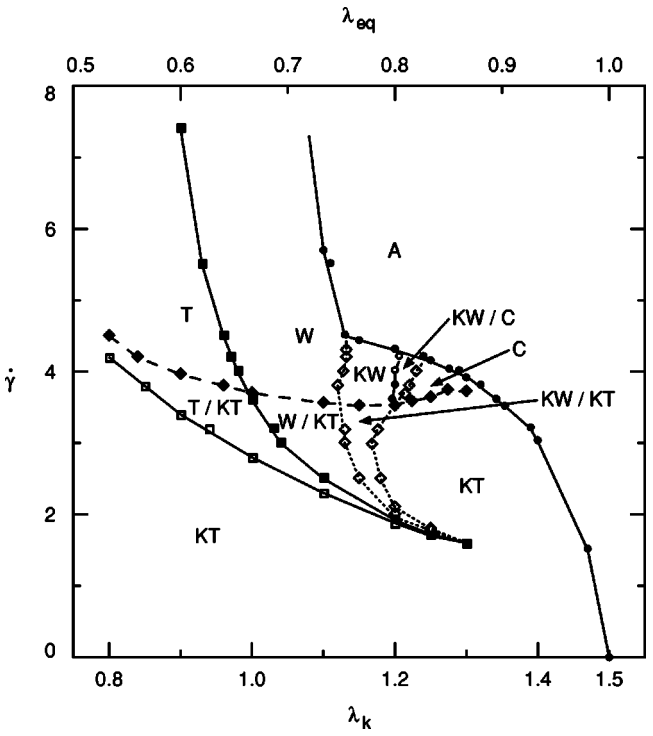

FIG. 1. Solution phase diagram of the steady and transient states of system (2), (3) for $\vartheta = 0$. The solid line is the border between the in-plane orbits *T*, *W*, and *A*; the dashed line and the dotted line delimit the regions where the out-of-plane orbits KT and KW, respectively, exist. Here $\dot{\gamma}$, λ_{eq}, and λ_k denote dimensionless shear rate, tumbling parameter of the Ericksen-Leslie theory, and $\lambda_k = \lambda_{eq}a_{eq}$ [see text part close to Eq. (2)].

Results are presented for $\vartheta = 0$, for $0.8 \leqslant \lambda K \leqslant 1.8$ (corresponding to $0.53 \leqslant \lambda_{eq} \leqslant 1.2$) and $0.1 \leqslant \dot{\gamma} \leqslant 10$. To obtain an overview of the possible orbits, the system (2), (3) was integrated numerically using a fourth-order Runge-Kutta method with fixed time step, starting from at least 10 random initial values of $a_0, \ldots, a_4$ for each combination of parameters. When the system had reached an asymptotic state (limit cycle or attractor), the domain of stability of this state in the parameter space was obtained by changing one parameter ($\dot{\gamma}$ or λ_k) in small steps and continuing the integration.

The following types of orbits, cf. Fig. 1, have been found tumbling (T): in-plane tumbling with $a_{3,4} = 0$; wagging (W): in-plane wagging with $a_{3,4} = 0$; aligning (A): in-plane flow alignment with $a_{3,4} = 0$; kayaking tumbling (KT): a periodic orbit with $a_{3,4} \neq 0$, where the projection of the director—the principal axis of $\mathbf{a}$ associated with the largest eigenvalue—onto the shear plane describes a tumbling motion; kayaking wagging (KW): a periodic orbit with $a_{3,4}$

$\neq 0$, where the projection of the director onto the shear plane describes a wagging motion, and complex (C): periodic orbits composed of sequences of KT and KW motion as well as aperiodic and chaotic orbits. The first three orbits T, W, and A were identified in Ref. [21]. The kayaking orbits [5] KT and KW are distinguished from each other according to Ref. [23]. Because Eqs. (2),(3) are invariant under the transformation $a_{3,4} \rightarrow -a_{3,4}$, two equivalent kayaking states exist.

A solution phase diagram of the various in-plane and out-of-plane states is drawn for $\vartheta = 0$ in Fig. 1. Though a detailed discussion about stability, coexisting, and transition states will have to be given elsewhere, we focus our attention to the region C, i.e., $\lambda K \approx 1.2$–1.3 and $\dot{\gamma} \approx 3.6$–4.2. The system shows rather complicated dynamical behavior in region C of the solution diagram, where neither one of the simple periodic states nor an aligning state is stable. The specific orbit depends on the parameters and the initial conditions. We are able to classify four categories of attractors:

(1) Periodic KT/KW composite state denoted by KTn/Wm: a state composed of n periods kayaking tumbling and m periods kayaking wagging, where $n = 0.5,1,1.5, \ldots$ and $m = 1,2,3$, etc. For higher shear rates, the KW sequences tend to be highly damped;

(2) Irregular KT or KT/KW state: a chaotic orbit consisting of either irregular KT oscillation or sequences of KT-type oscillation, irregularly interrupted by unsteady KW oscillations. The largest Lyapunov exponent is of order 0.01–0.05.

(3) Intermittent KT state: At the threshold to the irregular state for low λ_k and $\dot{\gamma}$, one has a large number of KT periods between the interruptions.

(4) Period-doubling KT states: Generally, the system exhibits a lot of more or less complicated periodic KTn/KWm states which are stable only within very small parameter intervals. The higher the values of n and m, the smaller is the stability interval. For certain values of the parameters, more than one KTn/KWm state exists. Between the stability regions of the periodic states, the behavior is chaotic, indicated by a positive largest Lyapunov exponent Λ_1. In many parts of the spectra, the chaotic regions are highly fragmented, which coincides with the observation of a large amount of periodic orbits spreading over the whole range of shear rates.

We observe that the route to chaos for increasing shear rates depends on the parameter λK: For $\lambda_k \leqslant 1.25$, one finds intermittent behavior for $\dot{\gamma}$ at the lower bound of region C. For $\lambda K = 1.26$, the KT state becomes metastable at $\dot{\gamma} = 3.7016$, where it coexists with a periodic KT3/KW1 or KT3.5/KW1 composite state, and chaos emerges either directly from the KT state at $\dot{\gamma} = 3.7025$ or from one of the above KT/KW composite states at $\dot{\gamma} = 3.7023$. For $\lambda_k = 1.27$ and greater, chaos emerges via a period-doubling route. When the flow-aligned (A) phase is approached from the complex (C) regime, the oscillation period grows infinitely high, in contrast to the behavior at the KW$\rightarrow$A transition, where the amplitude of the oscillation gets damped. But also in the latter case, the startup transients are modulated with a large-period oscillation. In order to determine the Lyapunov exponents, Eqs. (2),(3) and their linearizations were integrated from random initial variables and perturbation vectors using a fourth-order Runge-Kutta method. The integration time (shear strain) was $\dot{\gamma}t = 50\,000$, the transients up to $\dot{\gamma}t = 1000$ were ignored. If one estimates a kayaking-tumbling period to be of order $\dot{\gamma}t \approx 50$, the integration time corresponds to 1000 characteristic oscillation periods. The parallelepiped of perturbations was reorthonormalized every 20 integration steps, and the temporary Lyapunov exponents $\Lambda_i(t)$ were recorded periodically every 1000 shear strain units. The last value at $\dot{\gamma}t = 50\,000$ was taken as the result. Despite the limited exactness of their determination, the qualitative behavior of the largest Lyapunov exponent ($\Lambda_1 > 0$ or $\Lambda_1 = 0$) has been verified by testing the periodicity of the orbits at the selected shear rates.

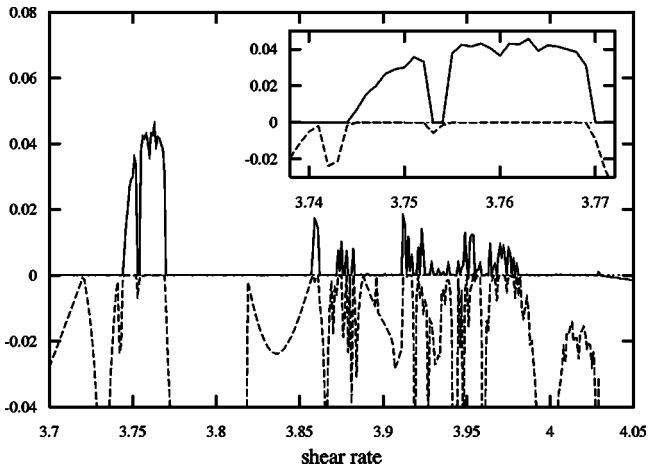

FIG. 2. The two largest Lyapunov exponents Λ_1, Λ_2 (solid and dashed line) of system (2), (3) for $\vartheta = 0$, $\lambda_k = 1.275$ as a function of $\dot{\gamma}$. The inset shows the beginning of the chaotic region in greater detail.

A selected Lyapunov spectrum for $\lambda K = 1.275$ is shown in Fig. 2. The error of the Lyapunov exponent Λ_1 was estimated to be $\delta\Lambda_1 = \pm 0.002 = \pm 6\%$. The occurrence of tran-

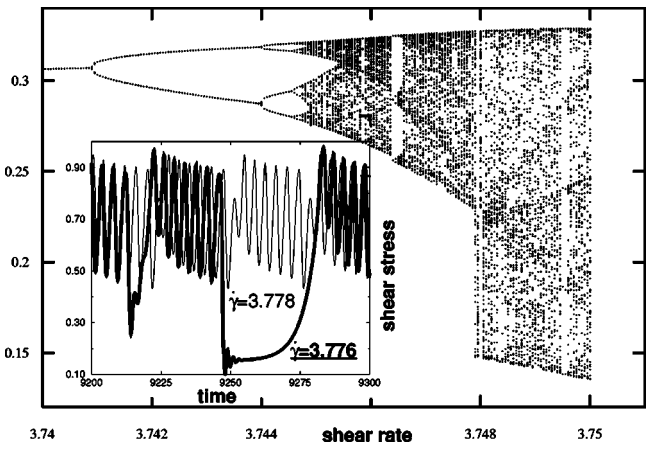

FIG. 3. Feigenbaum diagram of the period-doubling route of system (2), (3) for $\vartheta = 0$, $\lambda_k = 1.275$, and $\dot{\gamma} = 3.74$–3.75. Plot of the Poincaré map $a_4(t_i)$ for $i = 1$–82 at $a_3 = 0$ vs the "control parameter" $\dot{\gamma}$, the dimensionless shear rate. The inset shows the shear stress vs time for two fixed shear rates, $\dot{\gamma} = 3.778$ (thin line), and $\dot{\gamma} = 3.776$ (thick line), where the latter case exemplifies transient, rheochaotic behavior. All quantities in dimensionless units.

sient chaos for asymptotically periodic trajectories sometimes makes the analysis time consuming. Long transiently chaotic behavior was found within the integration time only 8 of 351 times for the particular set of parameters. For this selected value for λ_k, the system evolves towards chaos via successive period-doubling steps. At the first step, only the period of $a_0, \ldots, a_2$ is doubled. Then, with increasing $\dot{\gamma}$, the periods of all components are doubled. A bifurcation diagram, cf. Fig. 3, was constructed by computing the Poincaré map at $a_3=0$ for $\dot{\gamma}$ varied from 3.74 to 3.75 with step size 5×10^{-5}. The component a_4 at the times t_i where a_3 crosses zero is plotted in the diagram against the shear rate. The corresponding diagram for a_0 is very similar. Since the complex states always contain KT sequences with $a_{3,4}$ changing their sign twice every oscillation period, the hyperplane $a_3=0$ was taken as the Poincaré surface of section. The system was integrated up to $\dot{\gamma}t=6000$ and the transients for $\dot{\gamma}t<3000$ were skipped. As initial condition for the first value of $\dot{\gamma}$, a uniaxial **a** with equilibrium order parameter and the director given by the spherical angles $\phi=0$, $\theta=5/18\pi$ was used. For the remaining points, the integration was continued with increased $\dot{\gamma}$ using the end values of the preceding integration as initials. This was done to ensure that the system remains in the same oscillation state as long as possible: the states $(a_{3,4})$ and $(-a_{3,4})$ are chosen by the system depending on the initial conditions and lead to different Poincaré maps.

The resulting bifurcation plot has a striking similarity to the Feigenbaum diagram of the logistic map, $x_{n+1}=rx_n(1-x_n)$. The distance between successive period-doubling steps in Fig. 3 shrinks rapidly with the order of the period as in the Feigenbaum diagram. Even the chaotic region exhibits the same type of banded structure and has windows of periodic behavior. However, at $\dot{\gamma}\approx3.748$, the chaotic band enlarges abruptly. The reason for this behavior is the equivalence of the states $a_{3,4}$ and $-a_{3,4}$: both attractors were separated for $\dot{\gamma}<3.748$ and mix for $\dot{\gamma}>3.748$. To test the similarity of the period-doubling routes, the values $\dot{\gamma}_n$ where a period of order 2^n emerges and the value $\dot{\gamma}_\infty$ for the beginning of chaos were calculated for $n=1-5$ Like for the logistic map, the $\dot{\gamma}_n$ scale according to a law $\dot{\gamma}_n=\dot{\gamma}_\infty-C\delta^{-n}$ for $n\gg1$, with the Feigenbaum constant δ. A nonlinear fit yields $C=(0.0190\pm7)\times10^{-5}$ and $\delta=4.83\pm0.02$, The value agrees qualitatively with that for the logistic map. $\delta=4.669\ldots$, and a similar value had been reported in Ref. [8]. The Poincaré map in the chaotic regime for $\dot{\gamma}=3.7455$ is not shown here, but the plot of $a_0(t_{n+1})$ versus $a_0(t_n)$ has a single quadratic maximum, indicating the universal behavior. So the presence of the period-doubling route and the qualitative agreement of the value of the Feigenbaum constant δ receives an explanation. However, a side structure in the map growing with increasing shear rate prevents an oversimplified view of a full analogy.

In order to provide a link to rheological properties, we note that the symmetric traceless part of the stress tensor [16] associated with the alignment is $\bar{\boldsymbol{\sigma}}=nk_BTG\boldsymbol{\Sigma}$, with a dimensionless shear stress $\boldsymbol{\Sigma}\propto\lambda_k^{-1}\boldsymbol{\Phi}$ and a dimensionless shear modulus $G\propto\lambda_k^2\delta_K S_K^2$. Irregular behavior of the alignment tensor **a** will therefore immediately convert into irregular behavior for rheological properties, cf. Fig. 3, for an example. Based on the findings reported here, the inhomogeneous extension [17,24,25] of the present model can be expected to be of relevance in describing experimentally observed instabilities, and irregular banded and striped textures [11–14].

This research was supported in part by the National Science Foundation under Grant No. PHY99-07949 via the program ''Dynamics of complex and macromolecular fluids'' at the ITP, Santa Barbara, and it has been performed under the auspices of the Sonderforschungsbereich 448 ''Mesoskopisch strukturierte Verbundsysteme'' (Deutsche Forschungsgemeinschaft).

[1] J.L. Ericksen, Trans. Soc. Rheol. **5**, 23 (1961).
[2] G.B. Jeffrey, Proc. R. Soc. London, Ser. A **102**, 171 (1922).
[3] J. Mewis *et al.*, Macromolecules **30**, 1323 (1997).
[4] R.G. Larson, *The Structure and Rheology of Complex Fluids* (Oxford University Press, Oxford, UK, 1999).
[5] R.G. Larson and H.C. Öttinger, Macromolecules **24**, 6270 (1991); R.G. Larson, *ibid.* **23**, 3983 (1990); G. Marrucci and P.L. Maffettone, J. Rheol. **34**, 1217 (1990); P.L. Maffettone and S. Crescitelli, *ibid.* **38**, 1559 (1994).
[6] S. Hess, Z. Naturforsch. A **31a**, 1034 (1976).
[7] M. Doi, J. Polym. Sci., Polym. Phys. Ed. **19**, 229 (1981).
[8] M. Grosso *et al.*, Phys. Rev. Lett. **86**, 3184 (2001).
[9] A.L. Yarin *et al.*, J. Fluid Mech. **340**, 83 (1997).
[10] G. Rienäcker, *Orientational Dynamics of Nematic Liquid Crystals in a Shear Flow*, (Shaker Verlag, Aachen, 2000).
[11] R. Bandyopadhyay and A.K. Sood, Europhys. Lett. **56**, 447 (2002); R. Bandyopadhyay *et al.*, Phys. Rev. Lett. **84**, 2022 (2002).
[12] A.S. Wunenburger *et al.*, Phys. Rev. Lett. **86**, 1374 (2001).
[13] K. Satheesh Kumar and T.R. Ramamohan, J. Rheol. **39**, 1229 (1995).
[14] M.E. Cates, D.A. Head, and A. Ajdari (unpublished).
[15] O. Hess and S. Hess, Physica A **207**, 517 (1994).
[16] S. Hess, Z. Naturforsch. A **30a**, 728 (1975); C. Pereira Borgmeyer and S. Hess, J. Non-Equilib. Thermodyn. **20**, 359 (1995).
[17] S. Hess and I. Pardowitz, Z. Naturforsch. A **36A**, 554 (1981).
[18] M. Kröger *et al.*, J. Rheol. **37**, 1057 (1993); W. Muschik *et al.*, J. Non-Equilib. Thermodyn. **22**, 285 (1997); W. Muschik and B. Su, J. Chem. Phys. **107**, 580 (1997).
[19] S. Hess, Z. Naturforsch. A **31a**, 1507 (1976).
[20] P.D. Olmsted and P. Goldbart, Phys. Rev. A **41**, 4578 (1990); *ibid.* **46**, 4966 (1992).
[21] G. Rienäcker and S. Hess, Physica A **267**, 294 (1999).
[22] O. Hess and S. Hess, Physica A **207**, 517 (1994).
[23] N.C. Andrews *et al.*, J. Rheol. **40**, 459 (1996).
[24] G. Marrucci and F. Greco, Mol. Cryst. Liq. Cryst. **206**, 17 (1991).
[25] G. Sgalari *et al.*, J. Non-Newtonian Fluid Mech. **102**, 361 (2002).